2021 43rd Annual International Conference of the
IEEE Engineering in Medicine & Biology Society (EMBC)
Oct 31 - Nov 4, 2021. Virtual Conference

Towards Robust Control of PNS for Chronic Pain: Modeling Spinal Cord Wide-Dynamic Range Neurons with Structured Uncertainty

Christine Beauchene[1], Claire Zurn[1], Wanru Duan[2], Yun Guan[2], and Sridevi V. Sarma[1]

***Abstract*— Pain is a protective physiological system essential for survival. However, it can malfunction and create a debilitating disease known as chronic pain (CP), which is primarily treated with drugs that can produce negative side effects (e.g., opioid addiction). Peripheral nerve stimulation (PNS) is a promising alternative therapy; it has fewer negative side effects but has been associated with suboptimal efficacy since its mechanisms are unclear, and the current therapies are primarily open-loop (i.e. manual adjustment). To adapt to the needs of the user, the next step in advancing PNS therapies is to "close the loop" by using feedback to adjust the stimulation in real-time. A critical step in developing closed-loop PNS treatment is a deeper understanding of pain processing in the dorsal horn (DH) of the spinal cord, which is the first central relay station on the pain pathway. Mechanistic models of the DH have been developed to investigate modulation mechanisms but are non-linear, high-dimensional, and thus difficult to analyze. In this paper, we propose a novel application of structured uncertainty to model and analyze the nonlinear dynamical nature of the DH, and provide the foundation for developing robust PNS controllers using μ-synthesis. Using electrophysiological DH recordings from both naive and nerve-injured rats during windup stimulation, we build two separate models, which contains a linear time-invariant nominal (average) model, and structured uncertainty to quantify the nonlinear deviations in response from the nominal model. Using the structured uncertainty, we analyze the naive and injured models to discover underlying DH dynamics not identifiable using traditional methods, such as spike counting.**

I. INTRODUCTION

Acute pain is an early-warning signal, which is necessary for minimizing contact with painful, or noxious stimuli. However, chronic pain (CP) is a debilitating condition that occurs when the pain system malfunctions (e.g. from injury or disease). In the US, nearly 100 million adults are affected by CP [1]. The primary treatment for CP is pharmaceuticals, which have negative side effects (e.g., opioid addition), and lose efficacy after long-term use. A promising alternative treatment option is neuromodulation, such as peripheral nerve stimulation (PNS) or spinal cord stimulation (SCS), which uses brief pulses of electrical stimulation to modify activity in targeted nerves [2]. Currently, neuromodulation treatments produce fewer negative side effects but are associated with suboptimal efficacy since its mechanisms are unclear and the therapies are primarily open-loop (i.e. manual adjustment of stimulation parameters).

* This work is funded by the NIH/NINDS T32 NSO70201 to CB and NIH/NCCIH R01AT009401 to CZ, SVS, and YG.

[1]C. Beauchene, C. Zurn, and S.V. Sarma are with the Institute for Computational Medicine, Biomedical Engineering, Johns Hopkins University, Baltimore, MD, USA. (corresponding author: cbeauch2@jhu.edu)

[2] W. Duan and Y. Guan are with the Anesthesiology and Critical Care Medicine Department, Johns Hopkins University, Baltimore, MD, USA.

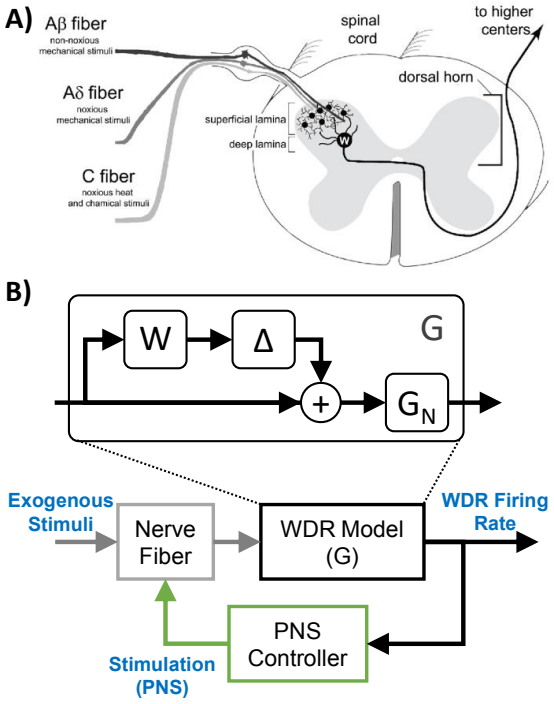

Fig. 1. A) Dorsal horn illustration. B) Closed-loop PNS system with the WDR neuron modeled with structured uncertainty. G_N and $W\Delta$ are the nominal LTI model, and the uncertain dynamics, respectively.

The next step in advancing PNS therapies is to "close the loop" by using feedback to adjust the stimulation in real-time. A critical step in developing closed-loop PNS treatment is a deeper understanding of pain processing in the dorsal horn (DH) of the spinal cord, which is the first relay station on the pain pathway (Fig. 1A). Primary afferent fibers transmit external sensory inputs to the DH. Wide-dynamic-range (WDR) neurons receive both noxious (Aδ and C fibers) and innocuous (Aβ fiber) inputs and plays a critical role by partially regulating the ascending pain transmission to the brain [3]. Electrophysiological recordings of the WDR neurons can provide important information about the dynamic pain processing changes due to CP.

One approach to developing closed-loop PNS therapies (Fig. 1B) is to build mathematical models of the DH [4]. However, modeling DH activity can be difficult due to the nonlinear components of the responses (i.e neuronal plasticity and sensitization). For example, during a windup input (repetitive brief pulses), Aβ fiber activation is relatively constant but the WDR neuronal responses to *C* fiber activation can change in a nonlinear fashion. This has led to mechanistic DH models, which can be high-dimensional and nonlinear, and thus hard to use for controller design [5], [6].

As a result, we propose a novel application of structured uncertainty that can then be used to build a robust PNS controller [7], [8]. As shown in Fig. 1B, we model the nonlinear WDR response with a linear time-invariant (LTI) nominal model (G_N) and structured uncertainty ($W\Delta$). Specifically, the nominal model predicts the average windup response across all input pulses. The structured uncertainty quantifies the amount of deviation (i.e. uncertainty) in response from the nominal model, across all windup pulses. As a proof of concept, we apply this powerful tool to electrophysiological DH recordings from both naive and injured rats to both model and analyze the nonlinear dynamical nature of the WDR response. From the structured uncertainty, we analyze the naive and injured models to find i) general characteristics across windup pulses, and ii) specific changes on individual pulses. This methodology leads to new understanding about the nonlinear DH dynamics, which are not identifiable using traditional methods (e.g. counting Aβ and C fiber spikes).

II. METHODS

A. Electrophysiology recordings of WDR neurons

Fine-tip microelectrodes are used to measure *in vivo* extracellular activity of the WDR neurons (Fig. 2A) from one naive and one spinal cord injured adult male rats (all procedures approved by the Johns Hopkins University Animal Care and Use Committee). Two windup trials (stimulation train of sixteen, 5mA, biphasic, and 0.5 ms pulses applied at 0.5Hz) per each animal [9].

We first identify the spikes by thresholding the data (recorded at 10kHz) at 4 times the standard deviation of baseline recordings. Next, to compute the firing rate, the binary spiking data is convolved with a 1,000-point Gaussian

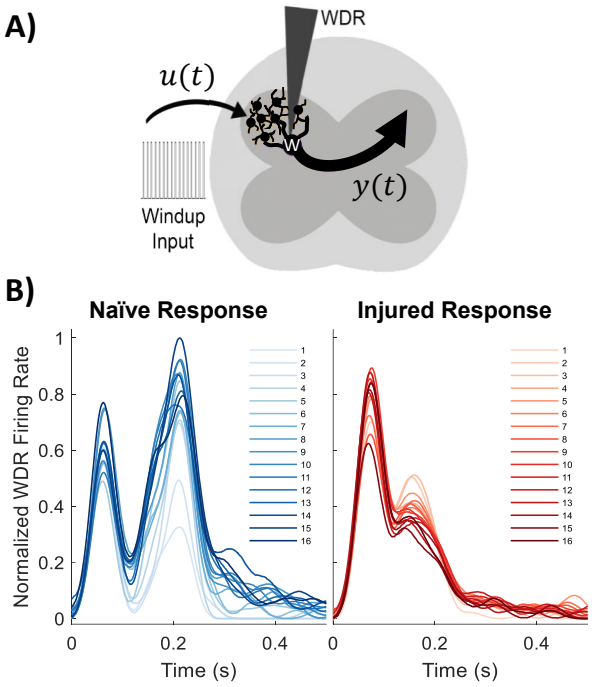

Fig. 2. A) A biophysical representation of the DH. The triangle is the recording microelectrode. The WDR neuron (W) projects to the brain. B) The normalized WDR firing rates, from the 16 pulses, for both conditions.

window. Next, each firing rate curve is normalized by its maximum value. Finally, the normalized firing rates, for both windup trials, are time-locked and averaged together. Fig. 2B shows firing rates of the WDR neurons in response to windup stimulation. We quantify these results by counting the number of spikes from the Aβ and the C-component.

B. Modeling WDR responses using structured uncertainty

Using structured uncertainty to model the WDR responses enables us to capture the nonlinearities and quantify the variations in dynamics across a windup input. To determine the model with structured uncertainty, we identify the range of windup responses by fitting an LTI model for each windup pulse. By dividing the response into 16 different models, we can achieve highly accurate model predictions. Also, we constrain the models to be linear to easily analyze the set of models and identify characteristics which are due to the windup pulse accumulation. We transform the set of models into an uncertain model by identifying the nominal model and the overall uncertainty in the model sets.

1) Identifying LTI models of WDR windup response: For both the naive and injured conditions, we fit 16 individual LTI continuous-time transfer function (TF) models to predict the WDR response for each of the windup pulse. We use the input, $u(t)$, and the WDR firing rate, $y(t)$, to estimate the TF, H, which is defined by

$$H(s) = \frac{a_0 s^z + a_1 s^{z-1} + a_2 s^{z-2} + \cdots + a_z}{b_0 s^p + b_1 s^{p-1} + b_2 s^{p-2} + \cdots + b_p} \quad (1)$$

where a_0 through a_z, and b_0 through b_p are fit using MATLAB. Specifically, two separate sets of models are fitted, one for the naive and one for the injured rat. We employ a search grid to identify the number of poles and zeros that produce the best response, across all 16 models. The number of zeros, z, ranged between 1 and 9, and the poles, p, ranged between 2 and 10, with $z < p$. We find the final zero - pole combination that produced the smallest root-mean-squared error (RMSE) and maximum absolute error (MAE), over all TF models. We quantify the final model results using the RMSE and MAE between the recorded and predicted responses.

2) Building WDR models with structured uncertainty: For this application, we model the structured uncertainty in the input multiplicative form (Fig. 1B), which is defined as the following set of transfer functions:

$$G = G_N(I + W\Delta) \quad (2)$$

We define the nominal system (G_N) to be the average TF over all 16 windup pulses. An additional TF (Δ) represents the uncertain dynamics with a unit peak gain. Finally, W is a fitted stable N^{th} order minimum-phase weighting function whose magnitude is greater than the largest relative error (between G_N and each model in the set). Therefore, W contains the amount of uncertainty in the potential windup responses, at all frequencies. For example, if the high frequency dynamics are not captured by the nominal model, then the weighting function acts as a high pass filter to reflect the frequencies with the largest amount uncertainty [7], [8].

III. RESULTS

A. Nonlinear windup characteristics

We first quantify these results of Fig. 2B by counting the number of spikes from the Aβ and the C fibers (Fig. 3). The naive rat shows a typical "windup" response where the amplitude of the second peak (C-fiber activation) generally increases with the number of pulses. The injured rat response is relatively consistent, potentially due to changes in spinal neuronal circuitry from the injury. This metric provides a good summary of the responses, but fails to fully capture the nonlinear dynamics observed during windup.

B. Predicting the windup response using LTI WDR models

Sixteen separate TF models are used to capture the dynamics of the WDR neurons in response to each windup input pulse. Based on the results of the search grids, the model sets with the best performance for the naive and the injured rat are seven zeros and nine poles, and three zeros and seven poles, respectively. Fig. 4 shows a comparison of the recorded WDR response and the model response, for the naive and the injured rat, for a selection of the windup pulses. For the recorded data, the thin solid line is the mean of the two windup trials, and the shaded region is the standard deviation. The darker, thick line is the predicted model response.

Fig. 5 shows the RMSE and MAE between the recorded WDR responses and the predicted model response, for both the naive and the injured conditions. Overall, the RMSE and MAE are small for both the conditions. However, for the naive models, we observe increased model error as the number of windup pulses increase, which is due to the constraint that each model must have the same order.

Also, we observe an interesting trend in the magnitude of the bode plots for each fitted TF model, which is particularly clear for the naive condition (Fig. 6). For each pulse, we see a similar magnitude-frequency response curve. However, we observe that the magnitude of the response increases with the number of windup pulses. This is a logical result based on the recorded responses, which also shows increasing C-fiber amplitude over the subsequent windup pulses.

C. Comparing WDR models with structured uncertainty

Lastly, for each condition, we build a model with structured uncertainty from the sets of TF models. The initial step is to identify the nominal models, G_N, for both the injured and naive rats. As we noted in the previous section, the set of models produced similar responses, but varied in magnitude. Therefore, for both sets of models, we chose G_N to be the average over the set of TF models. Fig. 7A shows the nominal responses (thick dotted lines) compared to the set of 16 responses (thin lines), for the naive and injured conditions. For both conditions, the nominal model response is the mean response across all 16 windup pulse responses.

Overall, the variation (i.e. uncertainty) in the set of naive models is greater than in the set of injured model. We can quantify the uncertainty by computing the relative error between the nominal model and each of the individual models in the set. Referencing the block diagram in Fig. 1B, we fit a

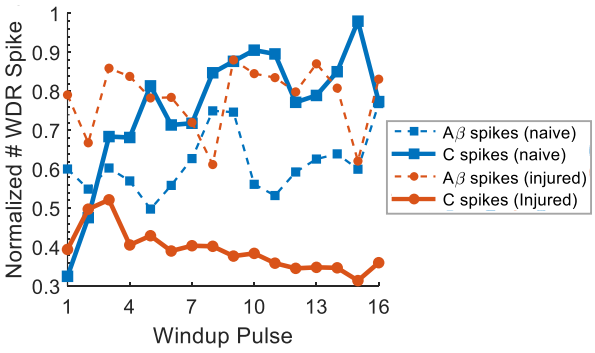

Fig. 3. Normalized spike counts for the Aβ and C fibers for both conditions

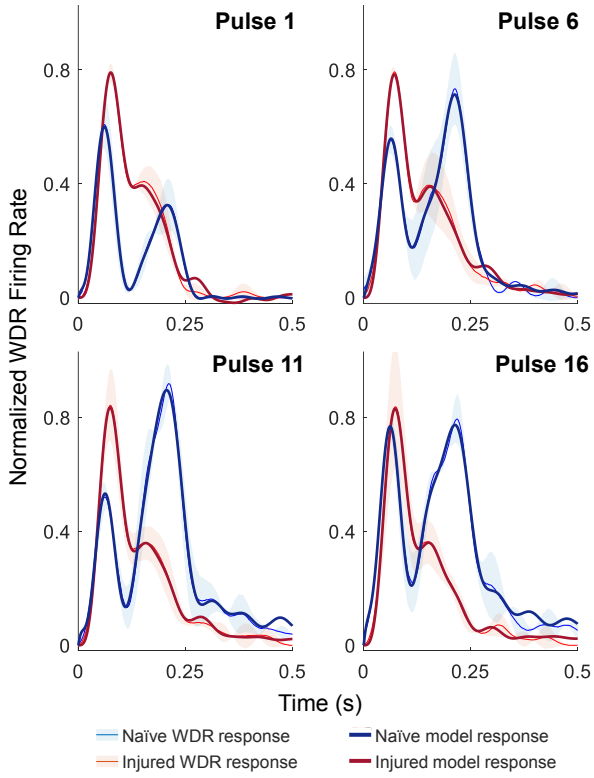

Fig. 4. A comparison of the predicted WDR firing rate responses and the recorded WDR responses for the naive and nerve-injured rat.

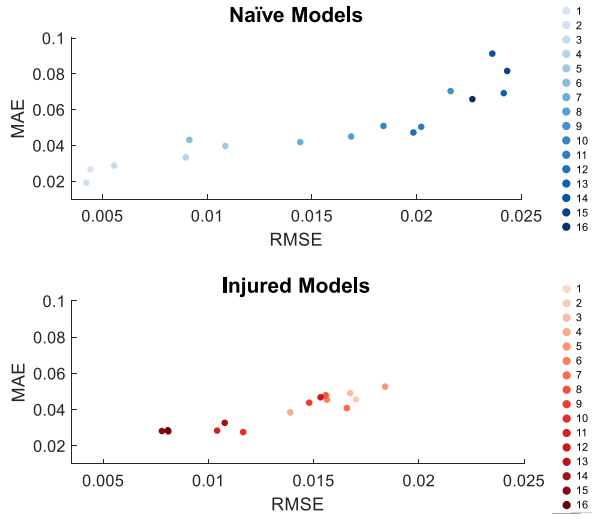

Fig. 5. The RMSE and MAE values for all 16 TF model predictions.

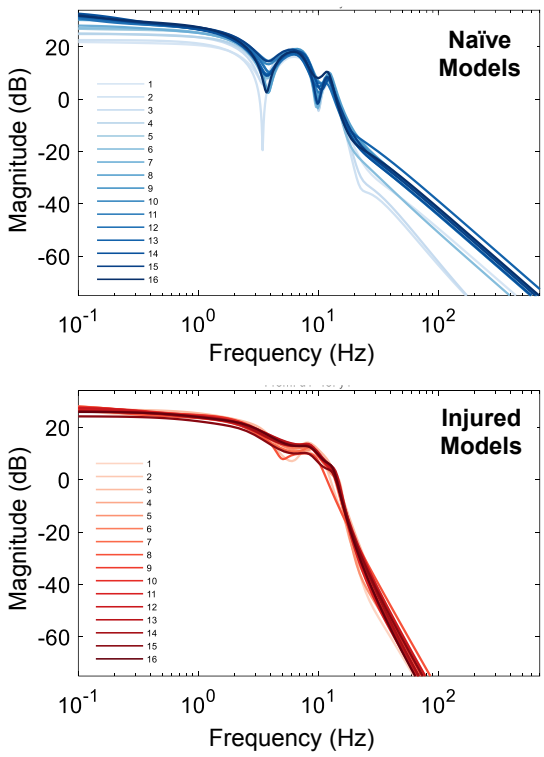

Fig. 6. Bode plots of all 16 fitted transfer function models.

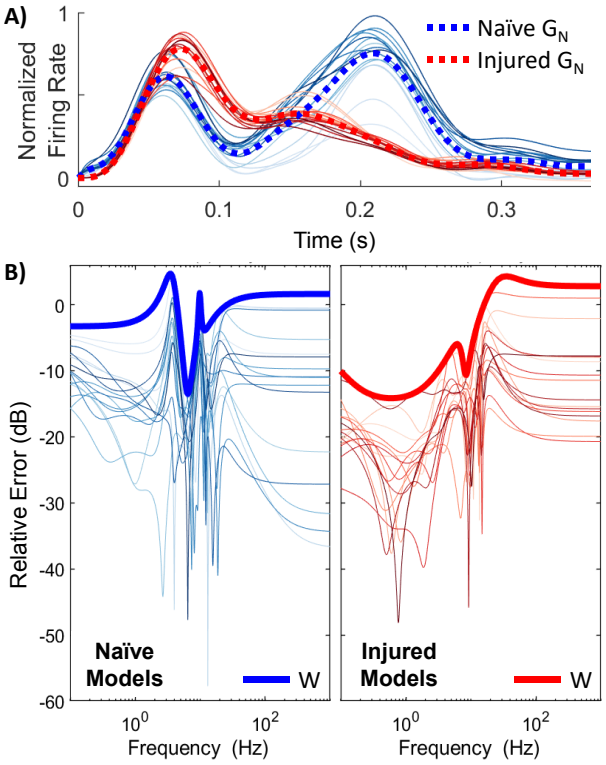

Fig. 7. A) WDR responses for each set of TF models, and the mean nominal model G_N. B) The relative error across the set of models, and the fitted uncertainty weighting function, W.

frequency-dependent uncertainty weighting function, W, by using the maximum relative error at each frequency, over the 16 responses, for both conditions. For this application, we chose a 5th order weighting function. In Fig. 7B, the dark thick lines indicate the weighting function, W, and the thin lines show the relative error between the nominal models (from Fig. 7A) and each of the 16 TF models in the sets.

By finding where the relative error and the uncertainty weighting functions is greater than 0dB, we can identify i) the range of frequencies where the variation is largest across all models in the set, and ii) specific windup pulse models that produce the largest variation for a particular frequency. For example, in the naive model, the greatest amount of variation, across all pulses, is between 2Hz - 5Hz and 8Hz - 11Hz. Additionally, we find that pulse 1 and pulse 16 varied the most at 4Hz and 10Hz, respectively. Alternatively, for the injured rat, the largest variation in responses occurs in frequencies higher than 25Hz, and the largest high frequency variations are observed in windup pulses 1, 3, and 8. Overall, using structured uncertainty is a powerful method for exploring the underlying dynamics of the DH that cannot be identified using traditional methods.

IV. DISCUSSION

In this paper, we use structured uncertainty to accurately model and analyze the dynamical nature of windup in the DH WDR neurons in naive and injured rats. The traditional analysis presented in Fig. 3 shows a good summary of the response. However, only after we fit a dynamical model with structured uncertainty (Fig. 7) are we able to identify the nonlinear changes in the DH, and be able to predict the response to novel inputs. The uncertain models developed in this work demonstrated the feasibility of these methods, and they will be applied to larger datasets in the future. The robust PNS controllers will depend on the identified structured uncertainty (i.e. low uncertainty leads to an aggressive controller, high uncertainty leads to conservative controller). We will use μ-synthesis to identify the robust PNS controller to drive the WDR response to improve CP treatment.

REFERENCES

[1] L. S. Simon, "Relieving pain in america: A blueprint for transforming prevention, care, education, and research," *Journal of Pain & Palliative Care Pharmacotherapy*, vol. 26, no. 2, pp. 197–198, 2012.

[2] Z. Chen, Q. Huang, *et al.*, "The impact of electrical charge delivery on inhibition of mechanical hypersensitivity in nerve-injured rats by subsensory threshold spinal cord stimulation," *Neuromodulation: Technology at the Neural Interface*, vol. 22, no. 2, pp. 163–171, 2019.

[3] D. J. Cavanaugh, H. Lee, *et al.*, "Distinct subsets of unmyelinated primary sensory fibers mediate behavioral responses to noxious thermal and mechanical stimuli," *Proceedings of the National Academy of Sciences*, vol. 106, no. 22, pp. 9075–9080, 2009.

[4] C. Beauchene *et al.*, "Modeling responses to peripheral nerve stimulation in the dorsal horn," in *41st Annual IEEE Engineering in Medicine and Biology Society Conference (EMBC)*, 2019, pp. 2324–2327.

[5] T. C. Zhang, J. J. Janik, *et al.*, "Modeling effects of spinal cord stimulation on wide-dynamic range dorsal horn neurons: influence of stimulation frequency and gabaergic inhibition," *Journal of Neurophysiology*, vol. 112, no. 3, pp. 552–567, 2014.

[6] F. Yang, Q. Xu, *et al.*, "Comparison of intensity-dependent inhibition of spinal wide-dynamic range neurons by dorsal column and peripheral nerve stimulation in a rat model of neuropathic pain," *European Journal of Pain*, vol. 18, no. 7, pp. 978–988, 2014.

[7] D.-W. Gu, P. H. Petkov, and M. M. Konstantinov, *Robust Control Design with MATLAB®*. Springer Science & Business Media, 2014.

[8] K. Zhou, J. C. Doyle, *et al.*, *Robust and Optimal Control*, vol. 40.

[9] W. Duan, Q. Huang, *et al.*, "Comparisons of motor and sensory abnormalities after lumbar and thoracic contusion spinal cord injury in male rats," *Neuroscience Letters*, vol. 708, p. 134358, 2019.